SUPPLEMENTAL MATERIAL

# NDF, a Nucleosome Destabilizing Factor that Facilitates Transcription through Nucleosomes

Jia Fei, Haruhiko Ishii, Marten A. Hoeksema, Franz Meitinger, George A. Kassavetis, Christopher K. Glass, Bing Ren, and James T. Kadonaga

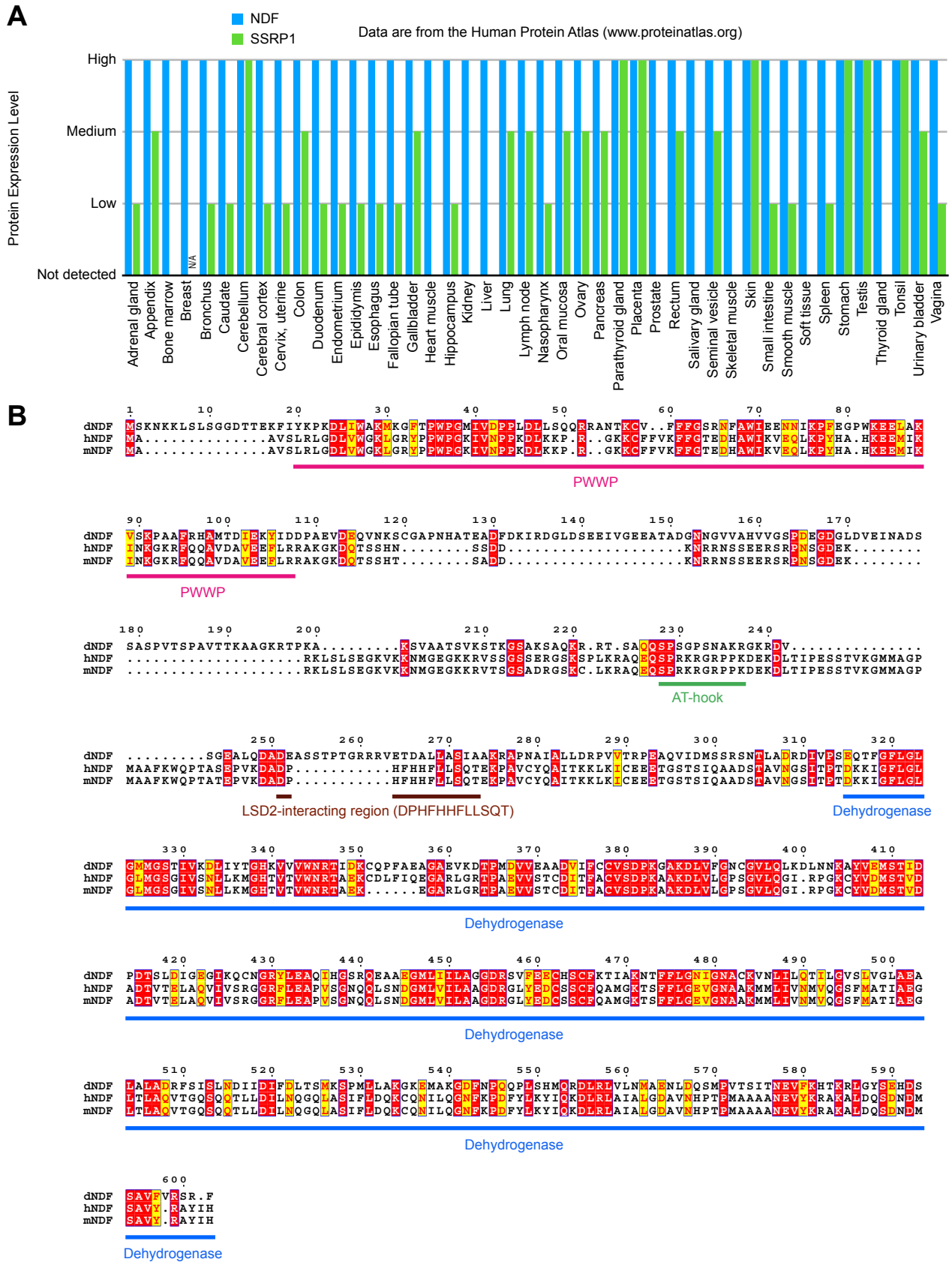


**Supplemental Figure S1.** Sequence and protein expression of NDF. (**A**) Protein expression levels of hNDF (GLYR1) and SSRP1 in 44 normal human adult tissues. DAB (3,3'-diaminobenzidine)-labeled antibodies were used for the immunohistochemistry experiments. The data were from www.proteinatlas.org. (**B**) Sequence alignment of *Drosophila*, human, and mouse NDF. These are the three versions of NDF that were examined in this study. The full-length sequences of dNDF (CG4747), hNDF, and mNDF (Glyr1) were aligned with T-Coffee (http://tcoffee.crg.cat/apps/tcoffee/do:regular). The resulting ClustalW file was converted into a PostScript file with ESPript 3.0 (http://espript.ibcp.fr/ESPript/ESPript/). Amino acid residues that are identical in the three proteins are highlighted in red, and amino acid residues with similar properties in all three proteins are highlighted in yellow. The locations of the PWWP domain, AT-hook motif, LSD2-interacting region, and dehydrogenase domain are shown. All three proteins contain the PWWP and dehydrogenase domains. The AT-hook and LSD2-interaction region are present in hNDF and mNDF, but not in dNDF. mNDF differs from hNDF by 14 amino acid residues.

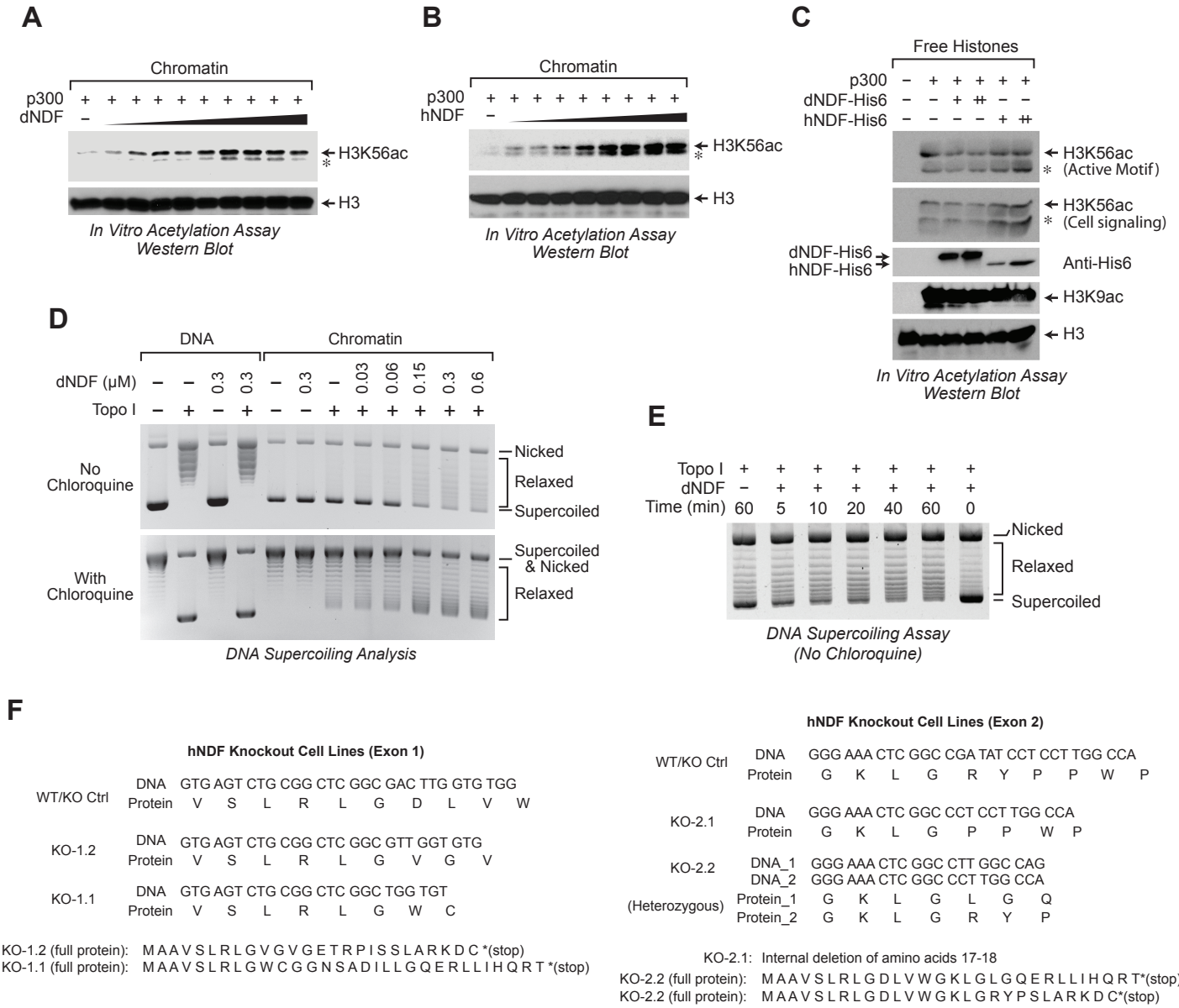


**F**

**hNDF Knockout Cell Lines (Exon 1)**

| | | |
|---|---|---|
| WT/KO Ctrl | DNA | GTG AGT CTG CGG CTC GGC GAC TTG GTG TGG |
| | Protein | V S L R L G D L V W |
| KO-1.2 | DNA | GTG AGT CTG CGG CTC GGC GTT GGT GTG |
| | Protein | V S L R L G V G V |
| KO-1.1 | DNA | GTG AGT CTG CGG CTC GGC TGG TGT |
| | Protein | V S L R L G W C |

KO-1.2 (full protein): M A A V S L R L G V G V G E T R P I S S L A R K D C *(stop)
KO-1.1 (full protein): M A A V S L R L G W C G G N S A D I L L G Q E R L L I H Q R T *(stop)

**hNDF Knockout Cell Lines (Exon 2)**

| | | |
|---|---|---|
| WT/KO Ctrl | DNA | GGG AAA CTC GGC CGA TAT CCT CCT TGG CCA |
| | Protein | G K L G R Y P P W P |
| KO-2.1 | DNA | GGG AAA CTC GGC CCT CCT TGG CCA |
| | Protein | G K L G P P W P |
| KO-2.2 | DNA_1 | GGG AAA CTC GGC CTT GGC CAG |
| | DNA_2 | GGG AAA CTC GGC CCT TGG CCA |
| (Heterozygous) | Protein_1 | G K L G L G Q |
| | Protein_2 | G K L G R Y P |

KO-2.1: Internal deletion of amino acids 17-18
KO-2.2 (full protein): M A A V S L R L G D L V W G K L G L G Q E R L L I H Q R T*(stop)
KO-2.2 (full protein): M A A V S L R L G D L V W G K L G R Y P S L A R K D C*(stop)

**Supplemental Figure S2.** Characterization of the activities of purified recombinant human and *Drosophila* NDF and generation of NDF knockout cell lines. (**A**) Analysis of the effects of different concentrations of recombinant dNDF in the acetylation of nucleosomal histone H3K56 by p300. Reactions were performed as in Fig. 2B of the main text in the presence of 0, 0.3, 0.6, 0.8, 1.1, 1.3, 1.4, 1.5, 1.7 or 1.8 μM dNDF with a nucleosome concentration of 1.4 μM. The asterisk denotes a nonspecific band. (**B**) Analysis of the effects of different concentrations of recombinant hNDF in the acetylation of nucleosomal histone H3K56 by p300. Reactions were performed as in Fig. 2B of the main text in the presence of 0, 0.3, 0.6, 0.8, 1.1, 1.3, 1.4, 1.5 or 1.7 μM hNDF. The asterisk denotes a nonspecific band. (**C**) Recombinant NDF does not stimulate the acetylation of H3K56 with free histones. Reactions were performed as in Fig. 2B of the main text, except that free histones were used instead of chromatin, with 1.4 $\mu$M core histone octamers, 0.7 $\mu$M (+) and 1.4 $\mu$M (++) dNDF, and 0.35 $\mu$M (+) and 0.7 $\mu$M (++) hNDF. (**D**) Destabilization of nucleosomes by dNDF. DNA supercoiling analysis of partial nucleosome disassembly by dNDF. Reactions with dNDF were carried out as with hNDF in Fig. 2D of the main text. (**E**) Time course of dNDF-mediated destabilization of chromatin. Reactions were performed as in **d** for the indicated times. (**F**) Genomic sequences of the human NDF (*GLYR1*) gene in wild-type and knockout (KO) cell lines. By using CRISPR-Cas9 methodology, four knockout cell lines were generated in HeLa cells by disruption of either exon 1 (KO-1.1 and KO-1.2) or exon 2 (KO-2.1 and KO-2.2) of the gene encoding NDF (*GLYR1*). For each cell line, the genomic DNA was purified, amplified by PCR, and sequenced. The proteins encoded by each of the cell lines are also indicated.

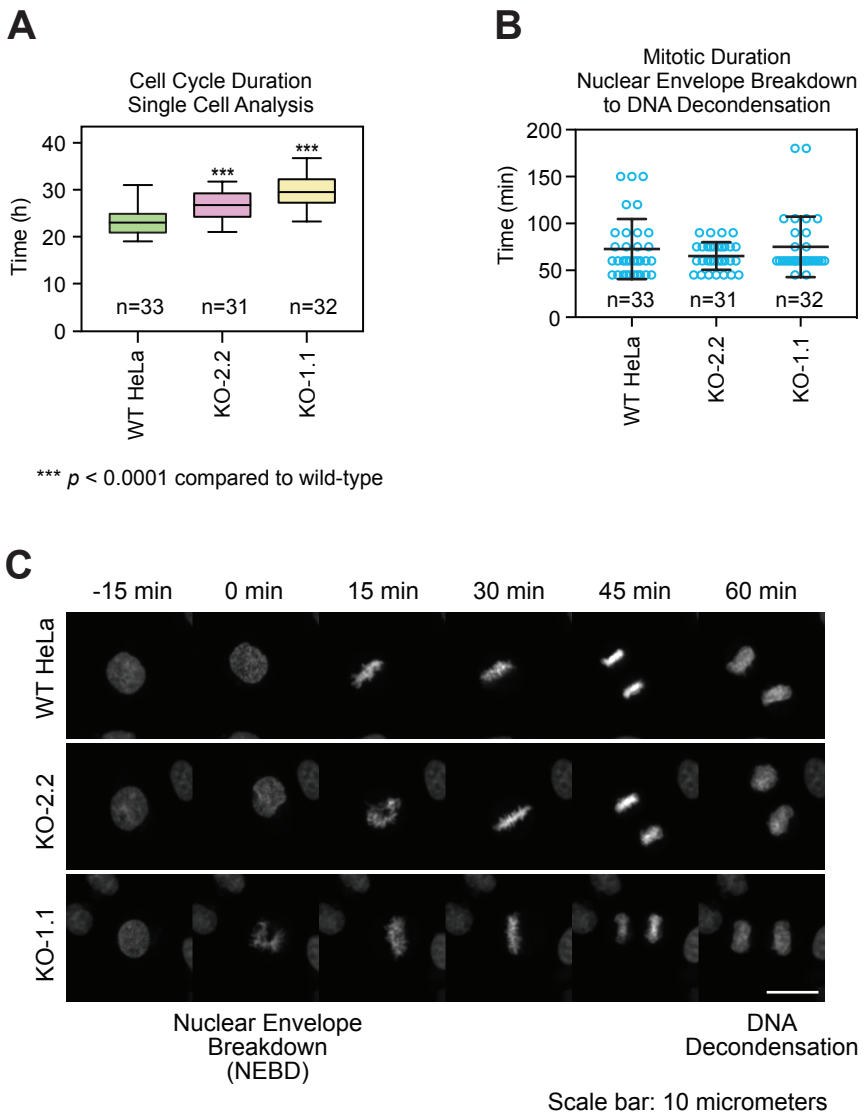


**Supplemental Figure S3.** Live-cell imaging analysis of wild-type and NDF knockout (KO) HeLa cells. (**A**) Single-cell cell cycle duration analysis. Both knockout cells exhibit an increase in the duration of the cell cycle relative to that in wild-type cells. (**B**) The duration of mitosis in NDF knockout cells is similar to that seen in wild-type cells. (**C**) Cell cycle imaging analysis reveals no apparent mitotic defects in NDF knockout cells.

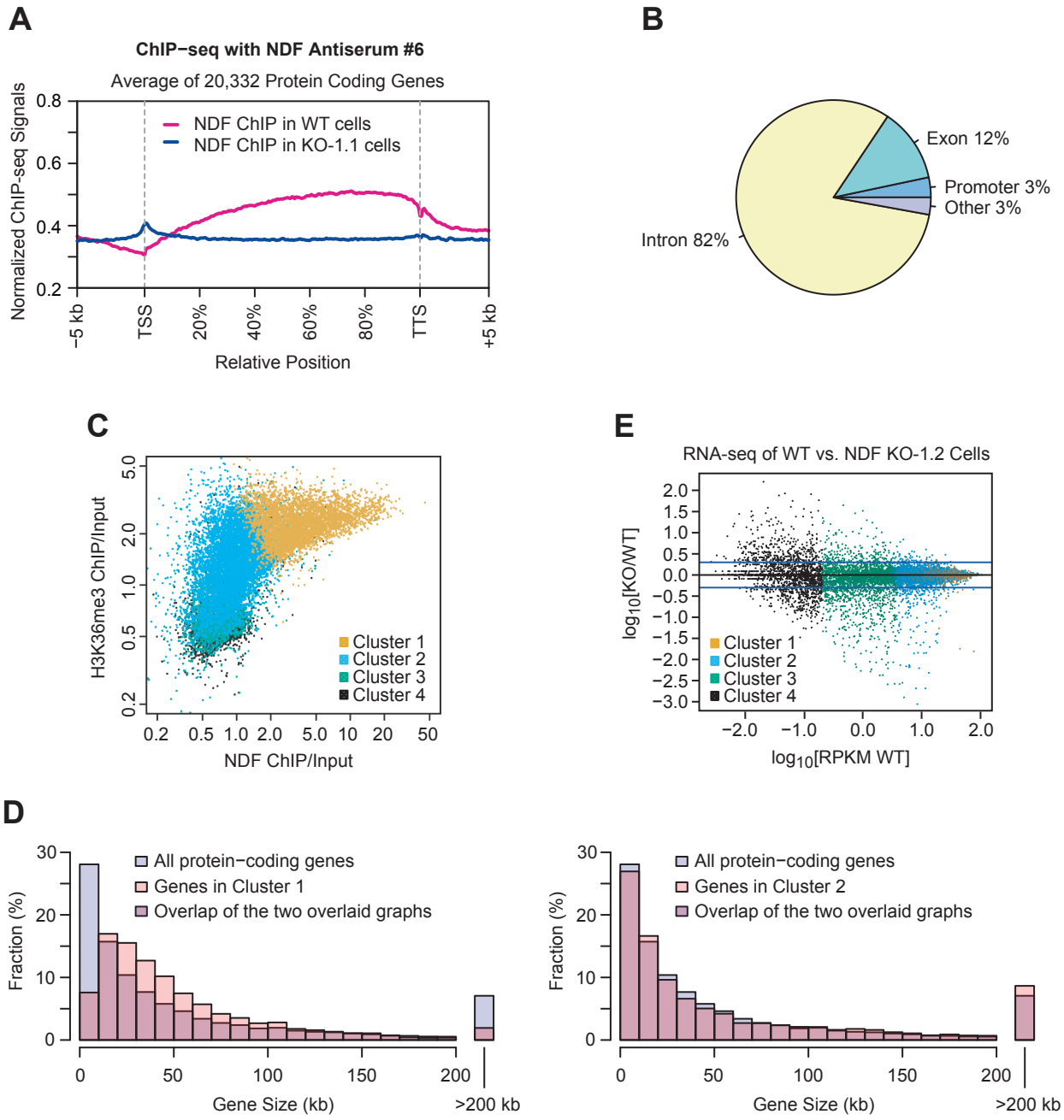


**Supplemental Figure S4.** Human NDF (hNDF) is enriched in transcribed regions of protein-coding genes with a preference for longer genes relative to shorter genes. (**A**) NDF is enriched in transcribed regions of protein-coding genes. Metagene analysis of NDF occupancy at 20,232 protein-coding genes with wild-type or NDF knockout (KO-1.1) HeLa cells. This experiment is similar to that shown in Fig. 3E of the main text, except that the data in this figure were generated with hNDF antiserum #6, whereas the data in main text Fig. 3E were generated with hNDF antiserum #7. (**B**) Genomic distribution of NDF ChIP-seq peaks in HeLa cells. Promoters were defined as regions that are +/– 200 bp from the transcription start site (TSS). (**C**) H3K36me3 is enriched in both active gene clusters 1 and 2. H3K36me3 ChIP/Input versus NDF ChIP/Input for gene clusters 1 to 4. The gene clusters were generated as described in Fig. 4 of the main text. (**D**) Active genes containing NDF (Cluster 1; left panel) are generally longer than active genes lacking NDF (Cluster 2; right panel). The gene clusters were generated as described in Fig. 4 of the main text. (**E**) RNA-seq analysis of wild-type versus hNDF KO-1.1 cells. The plot shows $\log_{10}$[(RPKM KO)/(RPKM WT)] versus $\log_{10}$[RPKM WT] for genes in clusters 1 to 4. Genes with RPKM = 0, such as those in cluster 4, were not incuded in this analysis. The upper and lower blue lines correspond to (RPKM KO)/(RPKM WT) ratios of 2 and 0.5, respectively.

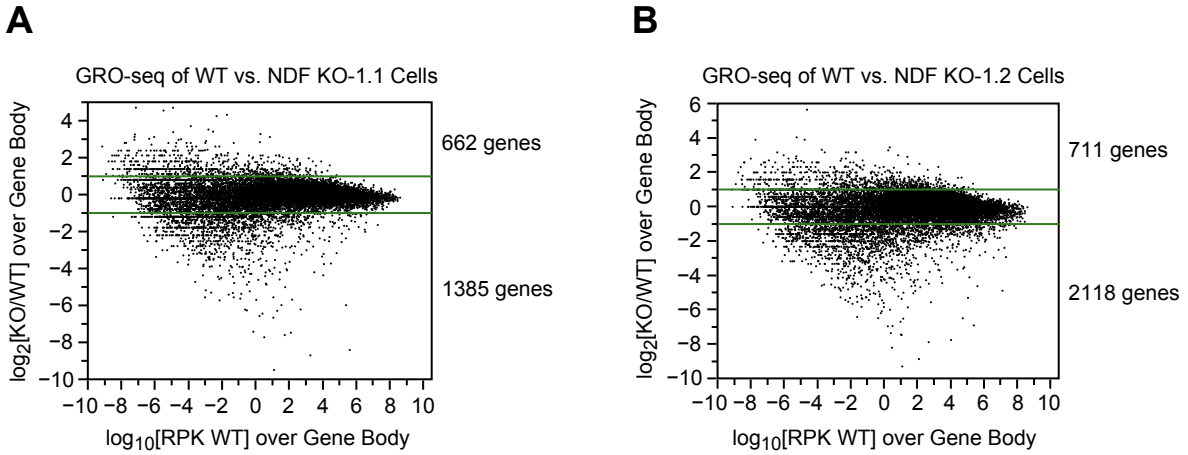


**Supplemental Figure S5.** GRO-seq analyses of wild-type and hNDF knockout (KO) cells reveal changes in Pol II dynamics upon loss of NDF. (**A**) Scatter plot of $\log_2$[(RPK KO)/(RPK WT)] versus $\log_{10}$[RPK WT] for genes in wild-type versus KO-1.1 cells. RPK is defined to be the reads per kilobase of gene body length (from the TSS to the TTS) per 10 million reads. The upper and lower green lines correspond to (KO/WT) ratios of 2 and 0.5, respectively. Out of 21,510 genes analyzed, there are 662 genes with at least a two-fold increase in the GRO-seq signal over the gene body and 1385 genes with at least a two-fold decrease in the GRO-seq signal over the gene body. (**B**) Scatter plot of $\log_2$[(RPK KO)/(RPK WT)] versus $\log_{10}$[RPK WT] for genes in wild-type versus KO-1.2 cells. Out of 21,287 genes analyzed, there are 711 genes with at least a two-fold increase in the GRO-seq signal over the gene body and 2118 genes with at least a two-fold decrease in the GRO-seq signal over the gene body.

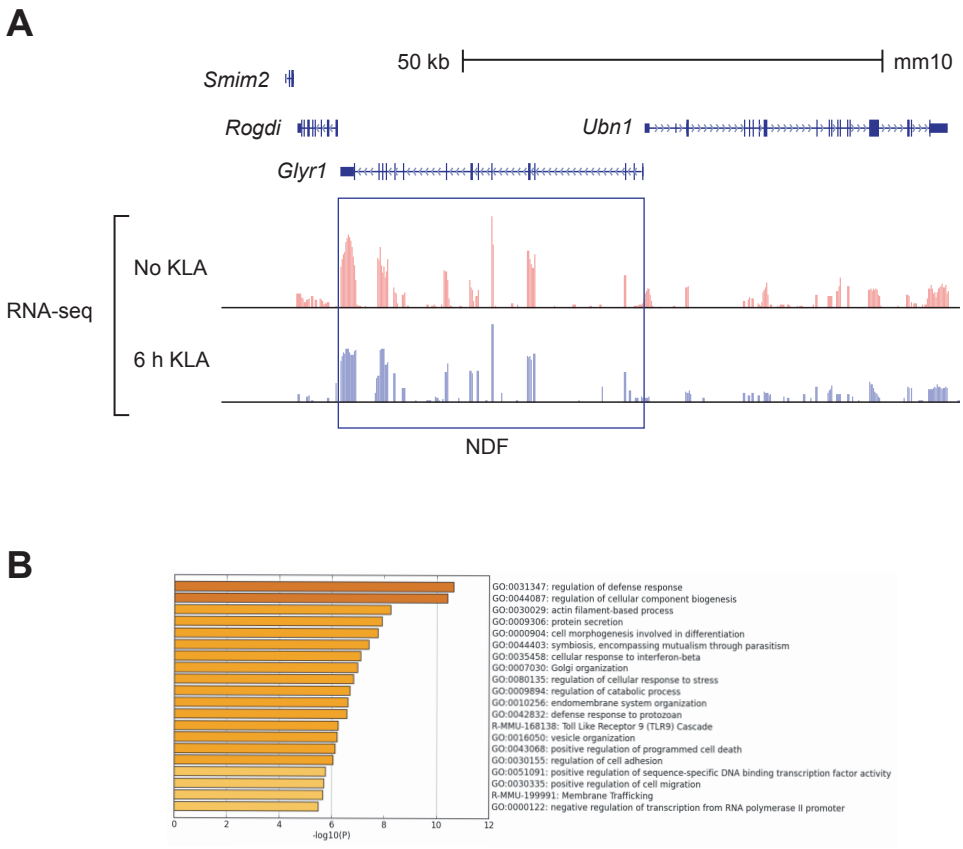


GO analysis of KLA-induced NDF peaks (6 h)

**Supplemental Figure S6.** Induction of mouse primary bone marrow derived macrophages (BMDM) by KLA. (**A**) Induction BMDM by KLA does not affect the expression of the *Glyr1* gene, which encodes mNDF. Genome-browser view of RNA-seq signal at the *Glyr1* gene with or without induction by KLA for 6 h. Transcripts in the region of the *Glyr1* gene are indicated by the box. (**B**) GO analysis of KLA-induced NDF peaks.

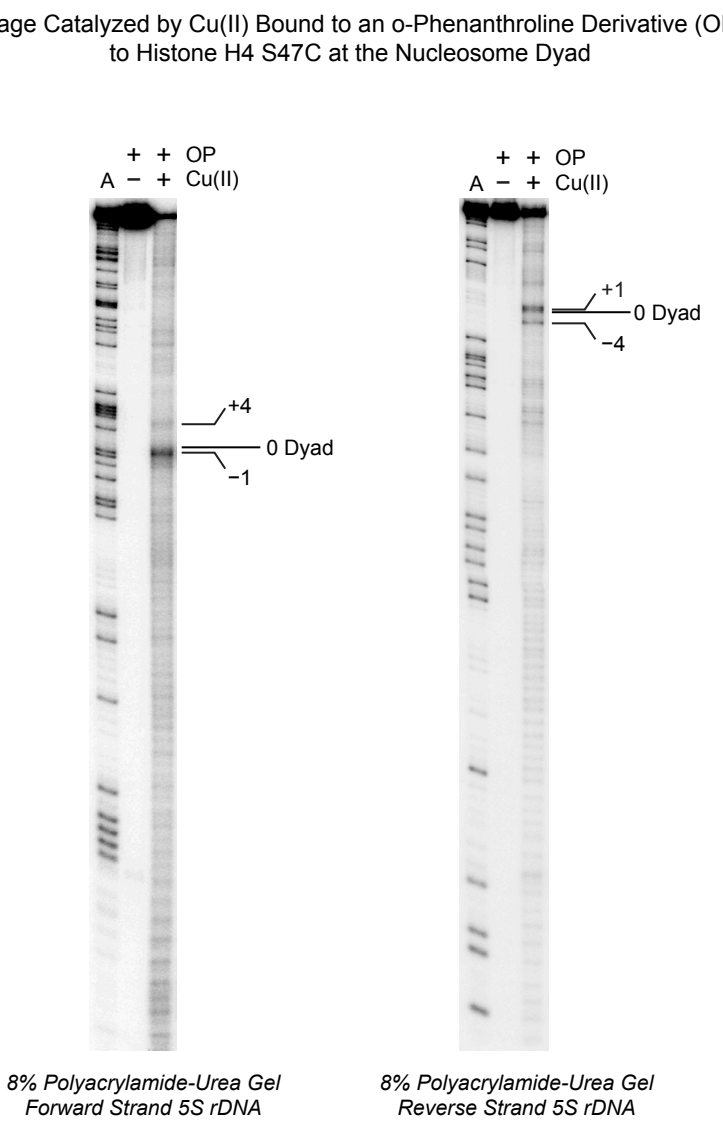


**Supplemental Figure S7.** Mapping the location of the dyad in nucleosomes positioned with the *Xenopus borealis* 5S rDNA sequence. Core histones containing H4S47C were modified with an o-phenanthroline derivative (OP), which links an o-phenanthroline moiety onto H4S47C via alkylation of the thiol group. The resulting derivatized histones were reconstituted into mononucleosomes by salt dialysis onto the forward or reverse strands of the *Xenopus borealis* 5S rDNA nucleosome positioning sequence. Hydroxyl radical cleavage reactions were initiated by the addition of Cu(II), hydrogen peroxide, and mercaptopropionic acid. The cleavage products were purified and analyzed by electrophoresis on an 8% polyacrylamide-urea gel. The Maxam-Gilbert A ladder was used to identify the OP cleavage products. The nucleosome dyad is located between the major and minor cleavage sites.

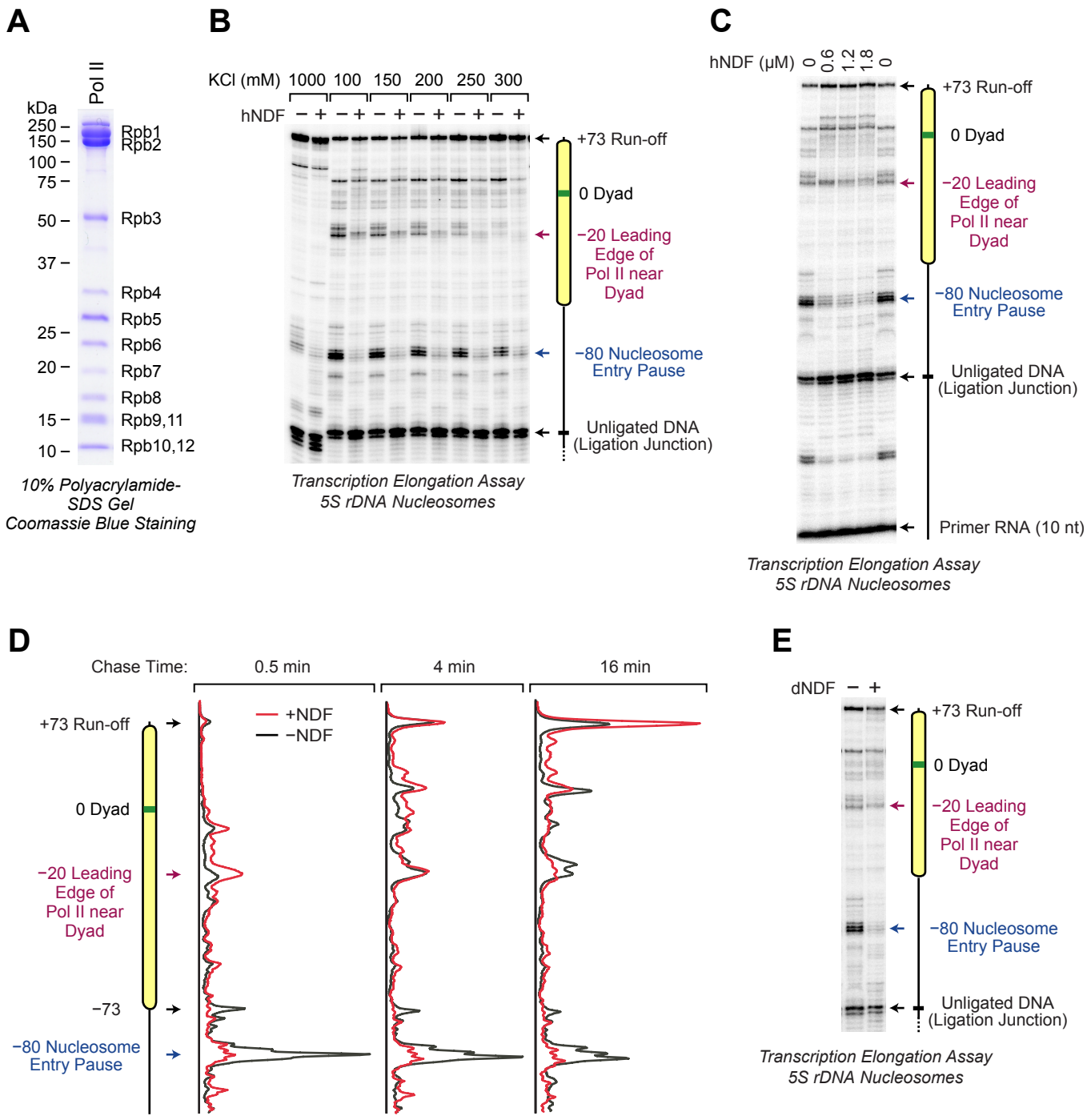


**Supplemental Figure S8.** Analysis of NDF in transcriptional elongation of Pol II through a nucleosome. (**A**) Purification of yeast RNA polymerase II (Pol II). The purified protein was analyzed by 10% polyacrylamide-SDS gel electrophoresis and staining with Coomassie Brilliant Blue R-250. (**B**) NDF stimulation of transcriptional elongation at different KCl concentrations. Reactions were performed with nucleosomal templates as in Fig. 6 of the main text (in which the KCl concentration is 100 mM) at the indicated concentrations of KCl for 6 min. hNDF was used at a concentration of 1.5 $\mu$M. As a reference/control, there is minimal inhibition of Pol II elongation upon dissociation of nucleosomes at 1000 mM KCl. (**C**) Effect of different concentrations of hNDF upon Pol II elongation through a nucleosome. Reactions were performed with nucleosomal templates as in Fig. 5 of the main text (in which the hNDF concentration is 1.5 $\mu$M) with the indicated concentrations of hNDF for 6 min. (**D**) Gel intensity scanning profile of Fig. 6B of the main text. Specifically, the 0.5 min, 4 min, and 16 min time points of Pol II elongation through nucleosomal templates are shown. (**E**) *Drosophila* NDF (dNDF) facilitates transcription elongation through nucleosomes. Reactions were performed with nucleosomal templates as in Fig. 5 of the main text for 4 min with dNDF (5 $\mu$M), where indicated.

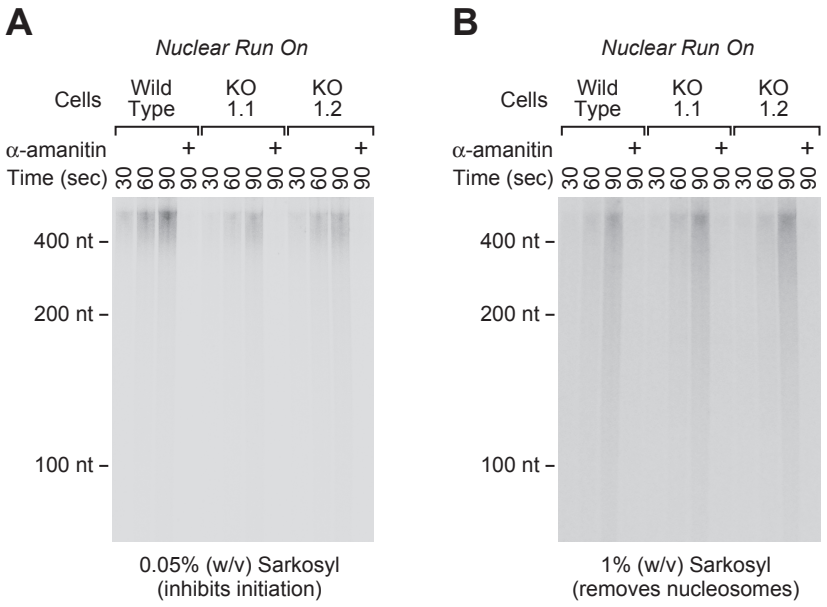


**Supplemental Figure S9.** NDF facilitates Pol II transcription elongation in chromatin in cell nuclei. (**A**) The loss of NDF results in a decrease in Pol II elongation in HeLa cell nuclei. Pol II run-on analysis was performed with nuclei from wild-type and NDF knockout cells. Nuclei were prepared from the indicated cells and incubated with α-$^{32}$P-labeled UTP and unlabeled ATP, CTP, and GTP in the presence of 0.05% (w/v) Sarkosyl to inhibit transcription initiation. The same number of nuclei were analyzed in each lane. Where indicated, α-amanitin was included at 4 $\mu$g/mL concentration to inhibit Pol II transcription. (**B**) The loss of NDF does not affect Pol II elongation in nuclei after removal of the histones from the DNA with 1% (w/v) Sarkosyl. Nuclear run-on experiments were performed as in A with 1% (w/v) Sarkosyl. Where indicated, α-amanitin was included at 4 $\mu$g/mL concentration to inhibit Pol II transcription.

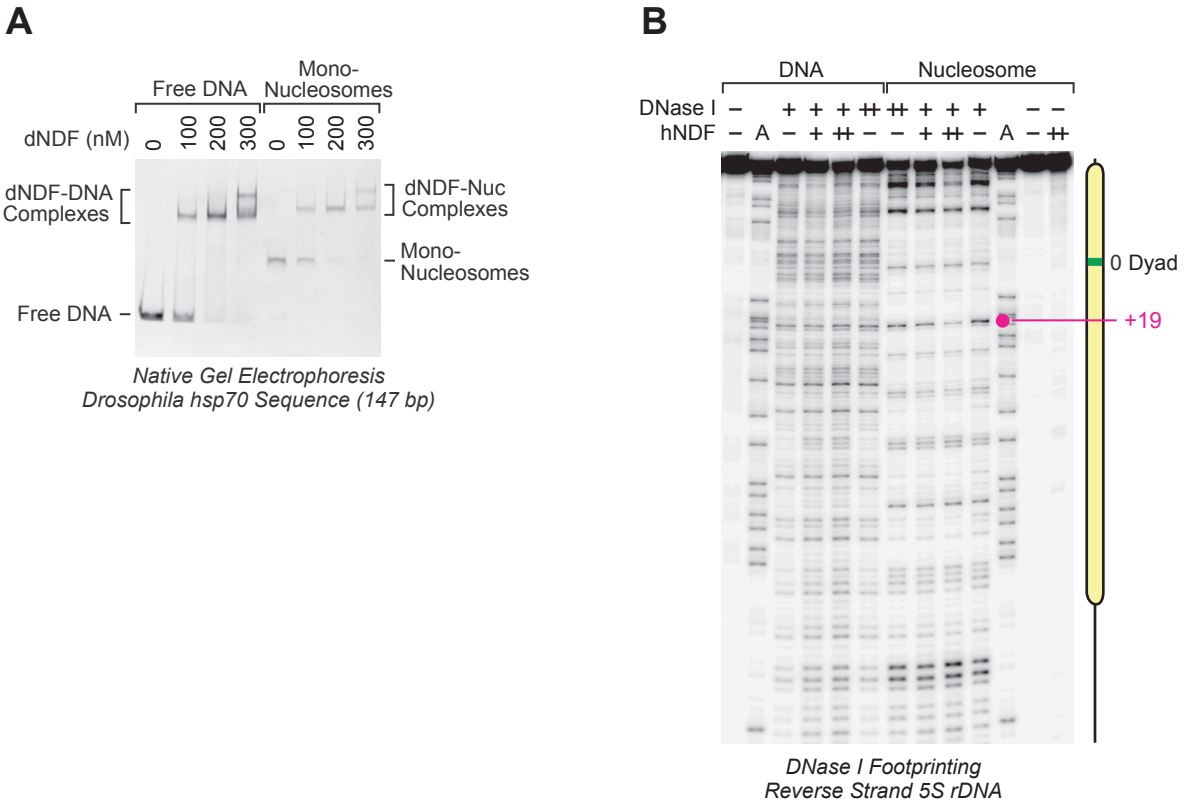


**Supplemental Figures S10.** Analysis of the binding of NDF to naked DNA and mononucleosomes. (**A**) *Drosophila* NDF (dNDF) binds to a *Drosophila hsp70* promoter DNA fragment as either mononucleosomes or free DNA. Gel mobility shift assays were performed with the indicated concentrations of dNDF and 50 nM of *Drosophila hsp70* promoter DNA (147 bp) as either naked DNA or mononucleosomes. The samples were incubated at 30˚C for 30 min and then subjected to electrophoresis on a 4% nondenaturing polyacrylamide gel. The DNA was visualized by staining with ethidium bromide. The positions of the shifted complexes are indicated. (**B**) DNase I footprinting analysis of hNDF with the reverse strand of *Xenopus borealis* 5S rDNA as either free DNA or mononucleosomes. DNase I footprinting reactions were performed as in Fig. 7B of the main text with the reverse strand of the 5S rDNA sequence (183 bp) as either naked DNA or mononucleosomes. Purified hNDF (73 nM or 150 nM concentration) was included where indicated. The Maxam-Gilbert A sequencing ladder was used to map the locations of the DNase I digestion products. The pink dot shows an NDF-protected nucleotide at +19 relative to the nucleosomal dyad at position 0.

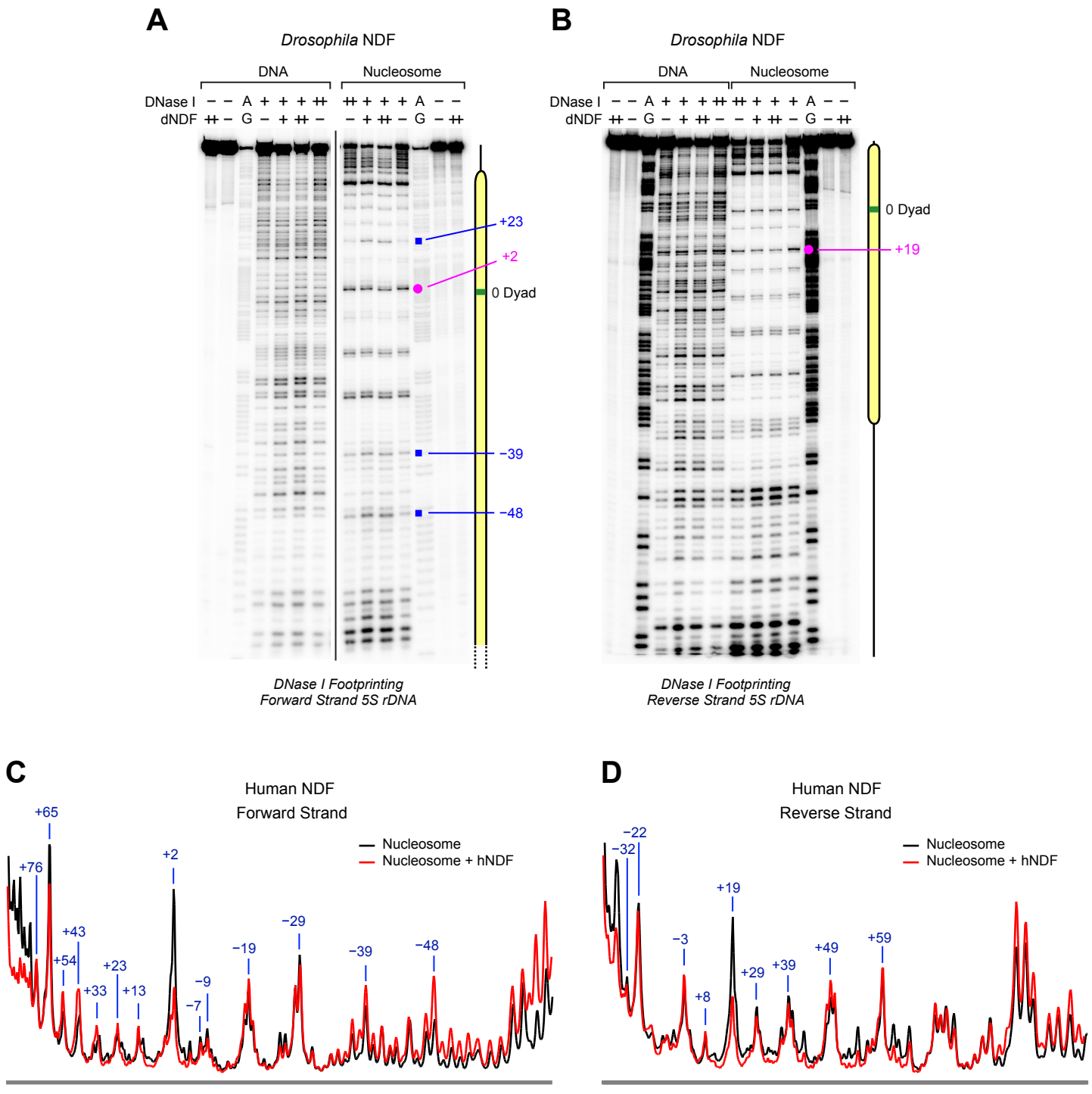


**Supplemental Figure S11.** DNase I footprinting analysis of the binding of NDF to naked DNA and mononucleosomes. (**A**) DNase I footprinting analysis reveals an interaction of dNDF near the nucleosome dyad. DNase I footprinting reactions were carried out with the forward strand of the 5S rDNA sequence (183 bp) as either naked DNA or mononucleosomes. Purified dNDF (0.35 $\mu$M or 0.7 $\mu$M concentration) was included where indicated. The Maxam-Gilbert A+G sequencing ladder was used to map the locations of the DNase I digestion products. The pink dot shows an NDF-protected nucleotide at +2 relative to the nucleosomal dyad at position 0. The blue squares designate bands that are enhanced in the presence of hNDF. (**B**) DNase I footprinting reactions, as in A, with the reverse strand of the 5S rDNA sequence. The pink dot shows an NDF-protected nucleotide at +19 relative to the nucleosomal dyad at position 0. (**C**) Gel intensity scanning profiles of the DNase I footprints of hNDF on mononucleosomes reconstituted with 5S rDNA. DNase I footprints with the forward strand, as shown in Fig. 7B of the main text. (**D**) Gel intensity scanning profiles of the DNase I footprints of hNDF with the reverse strand of 5S rDNA, as shown in Supplemental Fig. S10B.

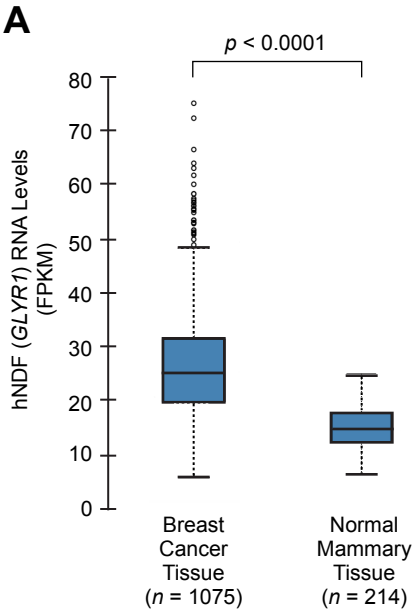


**B**

**Expression of hNDF (*GLYR1*)**

| Tissue | % Upregulated | % Downregulated | Number of patients tested |
|---|---|---|---|
| Adrenal gland | 15.19 | N/A | 79 |
| Breast | 21.19 | 3.62 | 1104 |
| Central nervous system | 3.87 | 4.88 | 697 |
| Cervix | 7.17 | 3.91 | 307 |
| Endometrium | 3.32 | 3.65 | 602 |
| Haematopoietic & lymphoid | 2.71 | 1.81 | 221 |
| Kidney | 5.67 | 1.83 | 600 |
| Large intestine | 6.56 | 2.62 | 610 |
| Liver | 2.41 | 9.65 | 373 |
| Lung | 4.61 | 6.38 | 1019 |
| Oesophagus | 4 | N/A | 125 |
| Ovary | 4.89 | 7.14 | 266 |
| Pancreas | 6.15 | 5.59 | 179 |
| Prostate | 1 | 5.82 | 498 |
| Skin | 5.29 | 4.65 | 473 |
| Soft tissue | 4.94 | 0.38 | 263 |
| Stomach | 3.16 | 4.21 | 285 |
| Thyroid | 2.92 | 3.9 | 513 |
| Upper aerodigestive tract | 4.02 | 6.13 | 522 |
| Urinary tract | 2.45 | 8.09 | 408 |

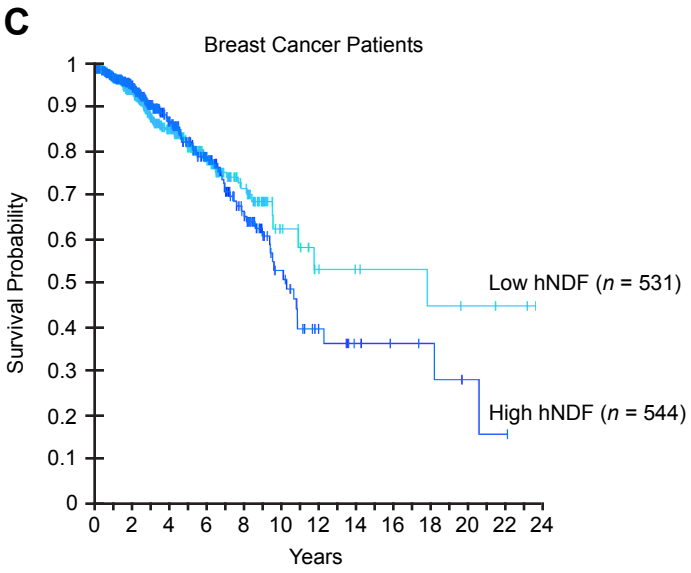


**Supplemental Figures S12.** hNDF (*GLYR1*) overexpression is frequently observed in breast cancer patients and appears to be an unfavorable prognostic marker. (**A**) hNDF expression levels (mRNA level, FPKM) in mammary tissues. The data are from The Human Protein Atlas (www.proteinatlas.org). (**B**) Altered expression of hNDF in different types of cancer. The data are curated by the Catalogue of Somatic Mutations in Cancer (COSMIC), Sanger Institute (cancer.sanger.ac.uk/cosmic). (**C**) Kaplan-Meier plot of breast cancer patients with high versus low levels of hNDF. The data are from The Human Protein Atlas (www.proteinatlas.org).

## Supplemental Materials and Methods

To ensure the reproducibility of the results, each experimental condition was performed independently at least two times.

### *Nucleic acid sequences*

The sequences of the nucleic acids used in this study are as follows.

*CRISPR-Cas9 targeting sequences for hNDF (GLYR1)*

Exon 1: GAGTCTGCGGCTCGGCGACT

Exon 2: AACTCGGCCGATATCCTCCT

Scramble/Control (from origene.com) : GCACTACCAGAGCTAACTCA

*Transcription elongation experiments*

Non-template strand (NTS) for transcription elongation experiments:

5’ Biotin-TGTCATCCCTTATGTGATGGACCCTATACGAATTCAGATATCGAGAGGACAGAAG GCGAAGAGCCAACCCAAGAGACACCGGCACTGGG-3’ [The 9 nt overhang for ligation of the TspRI-digested downstream sequence is highlighted in blue.]

Template strand (TS) for transcription elongation experiments:

5’-GGTGTCTCTTGGGTTGGCTCTTCGCCTTCTGTCCTCTCGATATCTGAATTCGTATAGGG TCCATCACATAAGGGATG-3’

RNA primer for transcription elongation experiments: 5’-AUCGAGAGGA-3’

[The Pol II elongation complex is assembled as follows. The 5' $^{32}$P-labeled RNA primer is hybridized to the template strand (TS), purified Pol II is added, and then 5'-biotinylated non-template strand (NTS) is added to give the Pol II elongation complex, which is then immobilized

onto streptavidin magnetic beads.]

Downstream sequence with the 5S rDNA nucleosome positioning sequence that is digested with TspRI and then ligated to the Pol II elongation complex:

CACATTAGGGCACTGGGTGGCACCGGCAAGGTCGCTGGGCCCGACCCTGCTTGGCTTCC
GAGATCAGACGATATCGGGCACTTTCAGGGTGGTATGGCCGTAGGCGAGCACAAGGCTGA
CTTTTCCTCCCCTTGTGCTGCCTTCTGGGGGGGGCCCAGCCGGATCCCCGGGCGAGCTC
GAATT

[The strand that is shown has the same sense as the non-template strand in the Pol II transcription experiments. This sequence is amplified by PCR, digested with TspRI, gel purified, reconstituted into a mononucleosome, and then ligated to the Pol II elongation complex. The underlined sequence is the central 146 bp of the 5S rDNA positioning sequence. The blue sequence is the TspRI restriction site.]

*DNase I footprinting and gel mobility shift experiments*

*Xenopus borealis* 5S rDNA sequence:

CATCCAAGTACTAACCAGGCCCGACCCTGCTTGGCTTCCGAGATCAGACGATATCGGGCA
CTTTCAGGGTGGTATGGCCGTAGGCGAGCACAAGGCTGACTTTTCCTCCCCTTGTGCTGC
CTTCTGGGGGGGGCCCAGCTCCTCCCCATGCCAGGGTCTTTTCCCCCAGGCAGGAAAACA
AGC

[This is the 183 bp sequence that was used in the DNase I footprinting experiments. The underlined sequence is the central 147 bp that was used in the gel mobility shift experiments.]

*Drosophila hsp70 (87A)* sequence:

AAATTTCTCTGGCCGTTATTCTCTATTCGTTTTGTGACTCTCCCTCTTTGTACTATTGCTCTC
TCACTCTGTCACACAGTAAACGGCGCACTGTTCTCGTTGCTTCGAGAGAGCGCGCCTCGA
ATGTTCGCGAAAAGAGCGCCGGAG

[This is the 147 bp sequence used in gel mobility shift experiments.]

***DNA supercoiling assay***

DNA supercoiling analyses were performed with either nucleosomes that were reconstituted onto plasmid DNA by salt dialysis (0.3 μM concentration of nucleosomes) or naked DNA as a reference along with the indicated concentrations of NDF, topoisomerase I (0.1 Units, as defined in ref. 42), and bovine serum albumin (1.4 μg) in Buffer S [25 mM Hepes, $K^+$, pH 7.6, 100 mM KCl, 0.2 mM $MgCl_2$, 0.1 mM EDTA, and 10% (v/v) glycerol] in a total volume of 50 μL. The mixture was incubated at 30˚C for 1 h. The reaction products were deproteinized, subjected to 0.8% agarose gel electrophoresis in the absence or presence of 10 ng/mL chloroquine, and stained with ethidium bromide.

***CRISPR-Cas9 knockout experiments***

Guide RNA sequences that target hNDF (*GLYR1*) exons 1 and 2 were designed by using crispr.mit.edu. The corresponding DNA sequences were subcloned into PX458 vector (gift from Gaoyang Liang, Salk Institute). The plasmids were transfected into HeLa cells by using Lipofectamine 2000 (Invitrogen) according the recommendations of the manufacturer. GFP-positive cells were collected and distributed into single cell clones in 96-well plates with a BD FACSAria II Sorter at the UCSD Stem Cell Core Facility. Individual clones were characterized by western blot analysis with anti-hNDF antibodies as well as by DNA sequencing (Ran et al. 2013).

***Cell cycle analysis***

For cell cycle analysis by flow cytometry, the cells were grown in 10 cm dishes. After dissociation with trypsin, 1 to 2 million cells were washed with PBS and resuspended in 300 μL of cold (4˚C) PBS. Cells were fixed by the dropwise addition of 0.8 mL of cold (4˚C) ethanol followed by incubation at 4˚C for a minimum of 24 h. After fixation, the cells were pelleted and

resuspended in 1 mL of PBS containing 50 µg/mL of propidium iodide and 10 µg/mL of RNase A. The cells were incubated for 30 min at 22˚C and then subjected to flow cytometry analysis. For each cell line, more than 50,000 cells were analyzed. For live cell imaging, 10,000 cells/well were plated in 96-well polystyrene plates 24h prior to imaging. The cells were stained with SiR-DNA dye (Spirochrome; used as recommended by the manufacturer) and imaged on the CQ1 spinning disk confocal system (Yokogawa Electric Corporation) with a 40x (0.95 NA) U-PlanApo objective and 2560x2160 pixel sCMOS camera (Andor) at 37°C and 5% $CO_2$. Image acquisition and data analysis were performed with CellVoyager software and ImageJ, respectively. 25 fields/well were imaged. 5 x 2 µm z-sections in far-red (25% power, 100 ms, binning 2) were acquired in each field at 15-minute intervals for 30 h.

***Nuclear run-on experiments***

Nuclei were isolated from wild-type and NDF knockout HeLa cells as follows. Except for the 1 x PBS, all buffers were at 4˚C. Cells in 15 cm dishes were washed three times with 1 x PBS and incubated with 10 mL of Swelling Buffer [10 mM Tris-HCl, pH 7.5, 2 mM $MgCl_2$, 3 mM $CaCl_2$, and 2 Units/mL Superase-in) on ice for 5 min. Cells were collected and resuspended in 0.5 mL of Swelling Buffer containing 10% (v/v) glycerol and 4 Units/mL Superase-In. One volume of IGEPAL Swelling Buffer [Swelling Buffer containing 10% (v/v) glycerol and 1% (v/v) IGEPAL CA-630 (Sigma)] was added, and the mixture was incubated on ice for 5 min. Cells were then washed once with 10 mL Lysis Buffer [Swelling Buffer with 0.5% (v/v) IGEPAL CA-630, 10% (v/v) glycerol, and 2 Units/mL Superase-In] and once with 1 mL Freezing Buffer [50 mM Tris-HCl, pH 7.5, 5 mM $MgCl_2$, 0.1 mM EDTA, 40% (v/v) glycerol, and 2 Units/mL Superase-In). The nuclei were resuspended at a concentration of 5 x $10^7$ nuclei/mL in Freezing Buffer.

The run-on experiments, which detect the elongation of transcriptionally-engaged Pol II in nuclei, were performed as follows. In each reaction, 10 µL of 3x Run-on Buffer [16.5 mM Tris-HCl, pH 7.5, 496 mM KCl, 8.25 mM $MgCl_2$, 1.5 mM DTT, 0.15% (w/v) Sarkosyl, 0.6 Units/µL Superase-In, 375 µM ATP, 375 µM GTP, 1.2 µM CTP and 27 nM $\alpha$-$^{32}$P-labeled UTP] was

added to 20 μL (1 x $10^6$) nuclei. The sample was gently mixed and incubated at room temperature for the indicated length of time (30, 60, or 90 s). The 0.05% (w/v) Sarkosyl was included to inhibit the initiation of Pol II transcription (Hawley and Roeder 1987).

To test Pol II elongation activity in the absence of nucleosomes, run-on reactions were performed in the presence of 1% (w/v) Sarkosyl, which removes the histones from the chromatin (Green et al. 1975; Scheer 1978). In these experiments, 3x Run-on Buffer containing 3% (w/v) Sarkosyl was used.

To test whether transcription was carried out by Pol II, α-amanitin was added, where indicated, to the nuclei to a final concentration of 4 ng/μL before the addition of the nucleotides. The run-on reactions were terminated by the addition of 150 μL Trizol LS (Invitrogen). The resulting radiolabeled transcripts were purified by chloroform extraction, precipitated with isopropanol, and analyzed by denaturing 6% polyacrylamide-urea gel electrophoresis. The gel images were collected on a GE Typhoon imager (GE Healthcare).

***DNase I footprinting***

The DNase I footprinting probes were generated by PCR of a 183 bp DNA fragment containing the 5S rDNA nucleosome positioning sequence with a 5'-$^{32}$P-labeled primer and an unlabeled opposite strand primer. The resulting single end-labeled DNA fragments were purified on a nondenaturing 6% polyacrylamide gel, and then reconstituted into nucleosomes by salt dialysis (Stein 1989; Fei et al. 2015). The efficiency of nucleosome reconstitution was estimated by nondenaturing 4% polyacrylamide gel electrophoresis, and samples with ≥95% nucleosome reconstitution were used for footprinting experiments. In a typical DNase I footprinting experiment, either mononucleosomes or corresponding naked DNA fragments (final concentration in 20 μL binding reaction is 14 nM) were incubated with the indicated concentrations of NDF in Buffer F [10 mM Hepes, $Na^+$, pH 7.8, 0.2 mM EDTA, 5% (v/v) glycerol, 100 mM NaCl, 5 mM $MgCl_2$ and 1 mM DTT] in a total volume of 20 μL at 30°C for 30 min. DNase I (Roche) was prepared freshly in DNase Dilution Buffer [40 mM Tris-HCl, pH 8.0, 5 mM

$MgCl_2$, 5 mM $CaCl_2$, and 1 mM DTT], and 2 µL was added to the reaction. The samples were quickly mixed and then incubated at 30˚C for 30 s. A final concentration of 1.0 or 1.5 mU/µL DNase I was used for the digestion of naked DNA, whereas a final concentration of 10 or 15 mU/µL was used for the digestion of chromatin. Reactions were terminated by the addition of 158 µL of Stop Buffer [10 mM Tris-HCl, pH 7.8, 3 mM EDTA and 0.2% (w/v) SDS]. The reaction products were extracted with phenol-chloroform, precipitated with ethanol, resuspended in formamide loading buffer, and subjected to electrophoresis on a denaturing 8% polyacrylamide-urea gel. The gel images were collected on a GE Typhoon imager (GE Healthcare).

***Mapping of the nucleosome dyad by H4S47C-directed cleavage***

To analyze the positioning of the nucleosomes, we used a modified version of the histone-directed DNA cleavage method of Flaus et al. (1996) with N-(1,10-phenanthrolin-5-yl)iodoacetamide (OP) as the histone H4S47C-alkylating reagent (Brogaard et al. 2012; Henikoff et al. 2014; Fei et al. 2015). We reconstituted nucleosomes with histone H4S47C, which is located near the nucleosome dyad, and the H4S47C was alkylated with OP, which resulted in a covalent linkage between the H4S47C thiol and an o-phenanthroline moiety. Then, upon addition of Cu(II) and hydrogen peroxide, the o-phenanthroline group mediated the generation of hydroxyl radicals that cleaved the nucleosomal DNA in the vicinity of the dyad. Specfiic reaction conditions are described in Fei et al. (2015).

***ChIP-seq analysis with HeLa cells***

For human NDF ChIP-seq, approximately 15 to 16 million cells (wild-type HeLa S3 cells or the indicated hNDF knockout cells) were collected and crosslinked with 1% formaldehyde (Sigma). The crosslinked cells were resuspended in 5 mL of Cell Lysis Buffer [5 mM Hepes, $K^+$, pH 8.0, 85 mM KCl, 0.5% (v/v) Nonidet P-40, and cOmplete, EDTA-free Protease Inhibitor Cocktail (Roche)]. The cells were incubated on ice for 5 min, and then pelleted by centrifugation at 500 x *g* at 4˚C for 5 min. The supernatant was removed, and the nuclear pellet was resuspended in

Nuclear Lysis Buffer [50 mM Tris-HCl, pH 8.0, 10 mM EDTA, 0.2% (w/v) SDS, and cOmplete, EDTA-free Protease Inhibitor Cocktail (Roche)] and then adjusted to a final volume of 1.2 mL. The resuspended sample was divided into four aliquots of ~300 µL in polystyrene tubes (Evergreen Scientific, 214-3710-010). Next, the samples were sonicated with a Qsonica Q800R sonicator with 70% amplitude and cycles of 30s on and 30s off for a total on time of 2 h. The samples were spun at 15,000 rpm (21130 x *g*) at 4˚C for 10 min, and the supernatant was collected. The samples were mixed with 1 x volume of Dilution Buffer [16.7 mM Tris-HCl, pH 8.0, 167 mM NaCl, 1.2 mM EDTA, 0.01% (w/v) SDS, 1.1% (v/v) Triton X-100, and cOmplete, EDTA-free Protease Inhibitor Cocktail (Roche)] and 0.5 x volumes 50% glycerol and then frozen in liquid nitrogen.

For immunoprecipitation, 300 µL of the sonicated sample and 200 µL of Dilution Buffer containing 0.25% (w/v) sodium deoxycholate were added to 20 µL of Dynabeads Protein A that were pre-bound with 1 µL of NDF antiserum. [Note that 1 µL of hNDF antiserum was optimal for hNDF antiserum #7. For hNDF antiserum #6, 2 µL was the optimal volume.] After incubation at 4˚C for 2 h on a nutating mixer, the tubes were placed on a magnetic stand, and the supernatant was removed. The beads were washed with 3 x 500 µL of Wash Buffer I [20 mM Tris-HCl, pH 7.5, 150 mM NaCl, 2 mM EDTA, 0.1% (w/v) SDS, 1% (v/v) Triton X-100], 3 x 500 µL of Wash Buffer II [10 mM Tris-HCl, pH 7.5, 250 mM LiCl, 1 mM EDTA, 0.7% (w/v) sodium deoxycholate, 1% (v/v) Nonidet P-40], and 1 x 500 µL of TET Buffer [10 mM Tris-HCl, pH 7.5, 1 mM EDTA, 0.1% (v/v) Tween-20] by resuspending the beads in the buffer and removing the supernatant on a magnetic stand. Next, the beads were resuspended in 100 µL of TET Buffer and transferred to new tubes. The supernatant was removed again, and the beads were resuspended in 50 µL of TE [10 mM Tris-HCl, pH 8, 1 mM EDTA] containing 1% (w/v) SDS for elution. The tubes were incubated at room temperature for 20 min and were placed on a magnetic stand to collect the eluate. Elution with 50 µL of TE containing 1% (w/v) SDS was repeated one more time. The eluates from both rounds were combined, and 6.4 µL of 5 M NaCl was added to adjust the final NaCl concentration to ~0.3 M. The samples were incubated at

65°C to reverse the crosslinks. After digestion with RNase A and proteinase K, the resulting DNA was isolated with MinElute columns (Qiagen). ChIP-seq libraries were prepared by end-repair, A-tailing, and ligation of Illumina TruSeq adaptors, which was then followed by PCR amplification and size selection with AMPure beads (Beckman Coulter). The libraries were sequenced with an Illumina Hi-Seq 4000 sequencer by using single-end 50 bp reads. The sequencing data were aligned to the hg19 reference genome by using Bowtie, and PCR duplicates were removed with the Picard tool (http://broadinstitute.github.io/picard/). Gencode Release 19 was used as gene annotation for the analysis.

***RNA-seq analysis with HeLa cells***

Total RNA was purified by using the PureLink RNA Mini RNA Kit (Thermo Fisher Invitrogen). The integrity of the RNA was measured by using the RNA 6000 Nano Kit with the Agilent Bioanalyzer 2100 system (Agilent Technologies). RNA-seq libraries were prepared with the TruSeq Stranded mRNA Library Prep Kit (Illumina). The libraries were sequenced with the Illumina Hi-Seq 4000 sequencer by using single-end 50 bp reads. The sequencing data were aligned to the hg19 reference genome by using the STAR RNA-seq aligner (Dobin et al. 2013), and PCR duplicates were removed with the Picard tool (http://broadinstitute.github.io/picard/). The reads that were assigned to genes were analyzed by using featureCounts (Liao et al. 2014) and gene annotation according to Gencode Release 19. The comparison of the wild-type cells versus the KO-1.1 and KO-1.2 cells was carried out three independent times.

***Global run-on sequencing (GRO-seq)***

GRO-seq was performed as described by Core et al. (2008). The data were mapped to the hg19 reference genome by using Bowtie2 (Langmead and Salzberg 2012). The resulting bam files were by analyzed by using HOMER (Heinz et al. 2010).

## Supplemental References


Brogaard K, Xi L, Wang JP, Widom J. 2012. A map of nucleosome positions in yeast at base-pair resolution. *Nature* **486**: 496-501.

Core LJ, Waterfall JJ, Lis JT. 2008. Nascent RNA sequencing reveals widespread pausing and divergent initiation at human promoters. *Science* **322**: 1845-1848.

Dobin A, Davis CA, Schlesinger F, Drenkow J, Zaleski C, Jha S, Batut P, Chaisson M, Gingeras TR. 2013. STAR: ultrafast universal RNA-seq aligner. *Bioinformatics* **29**: 15-21.

Fei J, Torigoe SE, Brown CR, Khuong MT, Kassavetis GA, Boeger H, Kadonaga JT. 2015. The prenucleosome, a stable conformational isomer of the nucleosome. *Genes Dev* **29**: 2563-2575.

Flaus A, Luger K, Tan S, Richmond TJ. 1996. Mapping nucleosome position at single base-pair resolution by using site-directed hydroxyl radicals. *Proc Natl Acad Sci* **93**: 1370-1375.

Green MH, Buss J, Gariglio P. 1975. Activation of nuclear RNA polymerase by Sarkosyl. *Eur J Biochem* **53**: 217-225.

Hawley D K, Roeder RG. 1987. Functional steps in transcription initiation and reinitiation from the major late promoter in a HeLa nuclear extract. *J Biol Chem* **262**: 3452-3461.

Heinz S, Benner C, Spann N, Bertolino E, Lin YC, Lasko P, Cheng JX, Murre C, Singh H, Glass CK. 2010. Simple combinations of lineage-determining transcription factors prime cis-regulatory elements required for macrophage and B cell identities. *Mol Cell* **38**: 576-589.

Henikoff S, Ramachandran S, Krassovsky K, Bryson TD, Codomo CA, Brogaard K, Widom J, Wang JP, Henikoff JG. 2014. The budding yeast Centromere DNA Element II wraps a stable Cse4 hemisome in either orientation in vivo. *eLife* **3**: e01861.

Langmead B, Salzberg SL. 2012. Fast gapped-read alignment with Bowtie 2. *Nat Methods* **9**: 357-359.

Liao Y, Smyth GK, Shi W. 2014. featureCounts: an efficient general purpose program for assigning sequence reads to genomic features. *Bioinformatics* **30**: 923-930.

Ran FA, Hsu PD, Wright J, Agarwala V, Scott DA, Zhang F. 2013. Genome engineering using the CRISPR-Cas9 system. *Nat. Protoc* **8**: 2281-2308.

Scheer U. 1978. Changes of nucleosome frequency in nucleolar and non-nucleolar chromatin as a function of transcription: an electron microscopic study. *Cell* **13**: 535-549.

Stein A.1989. Reconstitution of chromatin from purified components. *Methods Enzymol* **170**: 585-603.